Chapter 6: Distributed Octupole Lattice

This chapter discusses preliminary testing of a distributed octupole lattice, conducted in parallel with preparations for the more robust single-channel design.

6.1 Distributed Octupole Lattice Simulations

6.1.1 Variations of distributed lattice

6.1.2 Frequency Map Analysis

The idea of the distributed octupole lattice was first explored in the Elegant code, which allows beam tracking through third order matrices and symplectic elements. [**?**] Frequency map analysis shows the dynamic aperture is largest for an

# octupoles	spacing [m]	$\Delta\nu_x$	$\Delta\nu_y$
36	0.32	0.11	0.11
9	1.28	0.45	0.46
4	2.88	1.01	1.03

Tab. 6.1: Configurations considered for distributed octupole lattices. $\Delta\nu$ is tune advance between octupole centers in Elegant simulation.

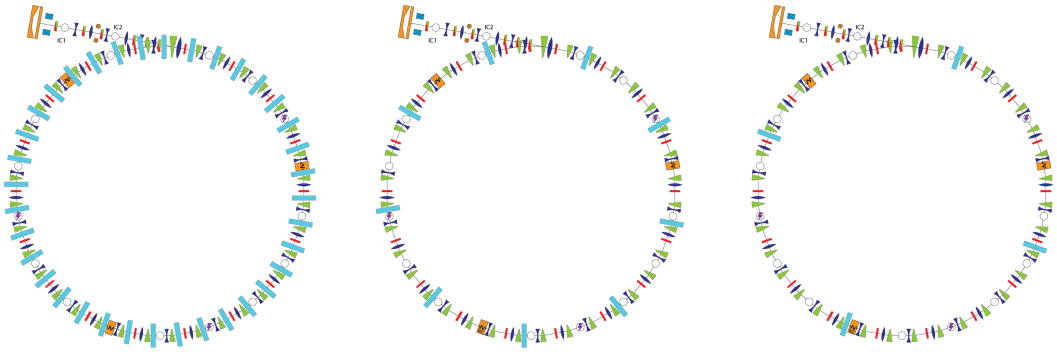

(a) N36 octupole lattice (b) N9 octupole lattice (c) N4 octupole lattice

Fig. 6.1: A selection of distributed octupole lattices tested for dynamic aperture and tune spread.

evenly distributed N4-octupole lattice With an octupole strength of $200T/m^3$, which corresponds to approximately 2.66 A in the physical octupoles, we see a tune shifts up to $\Delta\nu \approx 0.07$. This comes at the cost of operating near the integer resonance band.

The Elegant calculation was run at $\delta\psi_x = 1.06 * 2\pi$, $\delta\psi_y = 1.08 * 2\pi$ between octupoles (ring tune of $\nu_x = 4.45$, $\nu_y = 4.54$), slightly displaced from the ideal $\delta\psi_x = \delta\psi_y = 2\pi$ between octupoles. At this offset, the integer resonance band $\nu_x = \nu_y$ is visible in both configuration and tune space as an evacuated band, as seen in Fig. **??**. This integer band is destructive and cannot be mitigated by increasing octupole strength to drive up tune spread; The maximum externally induced tune spread is fixed, while the dynamic aperture decreases with octupole current (and amplitude dependent tunes scale accordingly).

A comparable analysis for single channel design was done in Elegant. The single channel octupole is expected to have a maximum tune shift of roughly twice

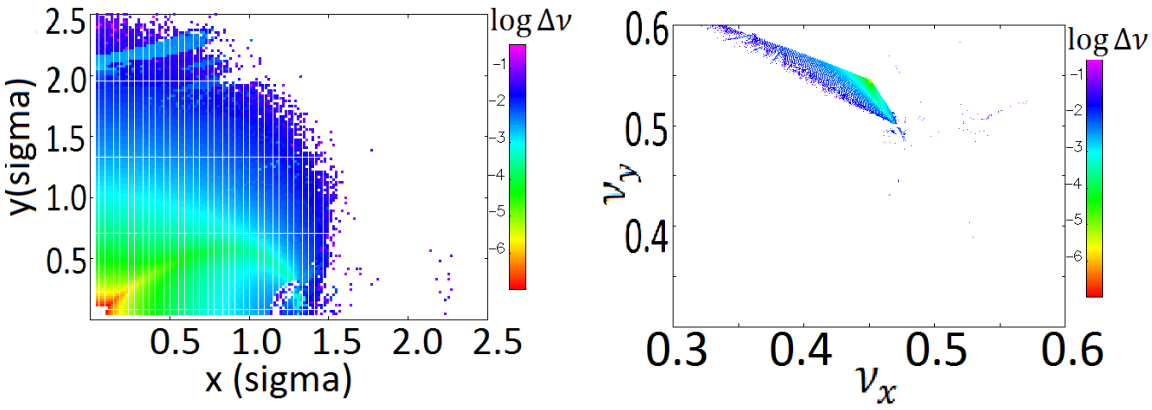

(a) (b)

Fig. 6.2: Frequency Map Analysis of N4 lattice in configuration and tune space

what is expected in the N4 lattice ($\delta\nu \approx 0.23$), and less apparent sensitivity to the $\nu_x = \nu_y$ band.

Tracking Hamiltonian Invariant

Simulations of N4 distributed lattices in the Elegant and Warp codes predict enhanced stability near the ideal tune operating point.

In comparison, invariant tracking through the N4 distributed lattice shows much larger amplitude oscillations in H_N, most likely due to the approximations on the nonlinear portion of the lattice. For the WARP model, we use hard edged elements in the alternative lattice configuration. Octupoles of length 5.2 cm and peak strength $75T/m^3/A$ are placed at 2.88 m intervals.

Two cases are considered: The historically utilized alternative lattice operating point $I_F = I_D = 0.87A$, which has a tune (as calculated in WARP) of $\nu_x = 3.88$, $\nu_y = 3.83$ and $I_F = 0.938A$, $I_D = 0.944A$, with tunes $\nu_x = 4.13$, $\nu_y = 4.11$. The two

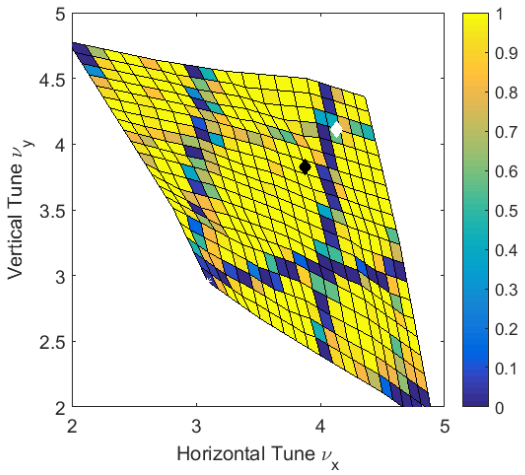

Fig. 6.3: Tune scan, simulated with WARP. Color axis shows particle survival over a range of operating points. Black marker indicates operating point $\nu_x = 3.88$, $\nu_y = 3.83$, while white marker indicates $\nu_x = 4.13$, $\nu_y = 4.11$.

operating points are marked in Fig. 6.3.

One expects the invariant to be perfectly conserved in the linear case ($I_{oct} = 0$). Also, decrease of dynamic aperture with increasing octupole strength is can be seen through high-amplitude unstable chaotic orbits leaving the system. Recall, for the nonlinear invariant to be conserved, particles must have continuous motion through the octupole elements otherwise chaotic, unbounded orbits are permitted. [1] In the case continuous motion (or quasi-continuous, allowing for linear inserts between octupoles) cannot be maintained, we expect the invariant quantity to be less bounded. As seen Fig. 6.4 and Fig. **??**, particles seem to gain stability as the external focusing nears the $\nu_x = \nu_y = 4.07$ condition. However, simulations at this operating point yield poor results, and the invariant is not well conserved.

While the Hamiltonian is not well conserved, long term stability (past the

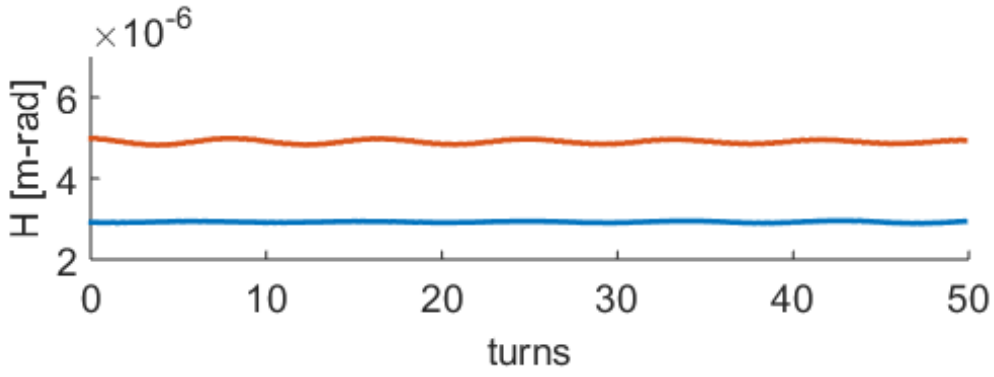

(a)

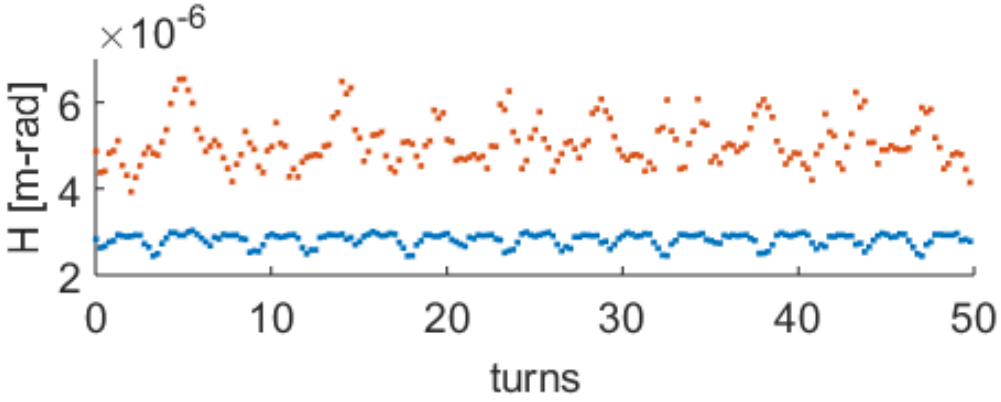

(b)

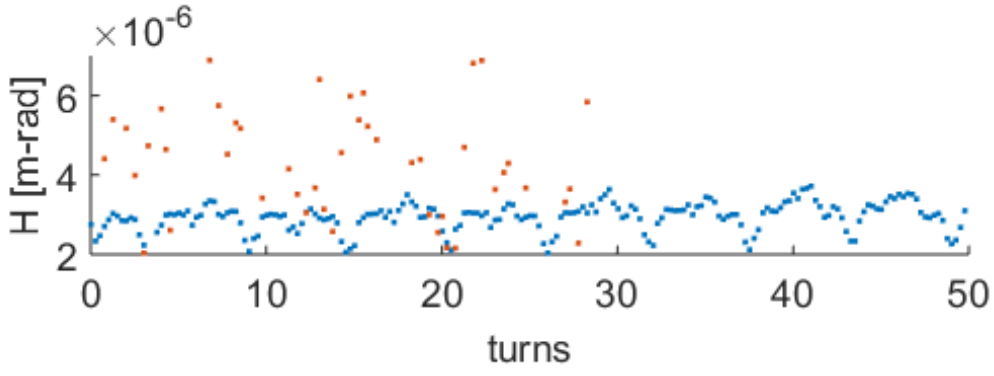

(c)

Fig. 6.4: Invariant H_N for N4 distributed lattice at $\nu_x = 3.88$, $\nu_y = 3.83$

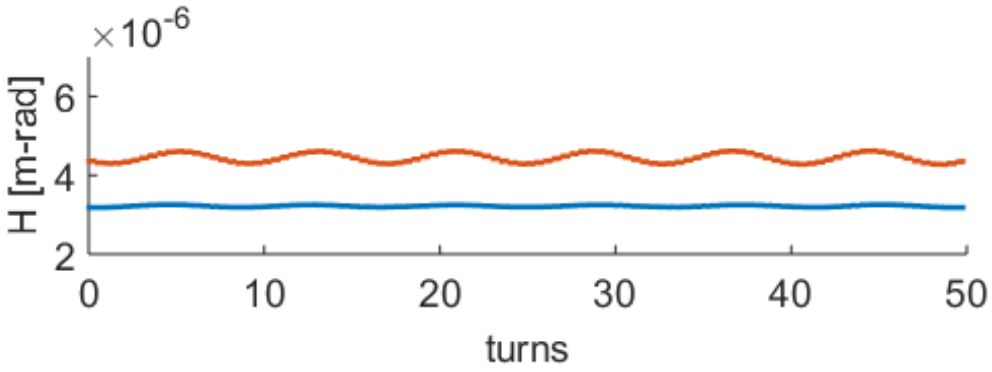

(a)

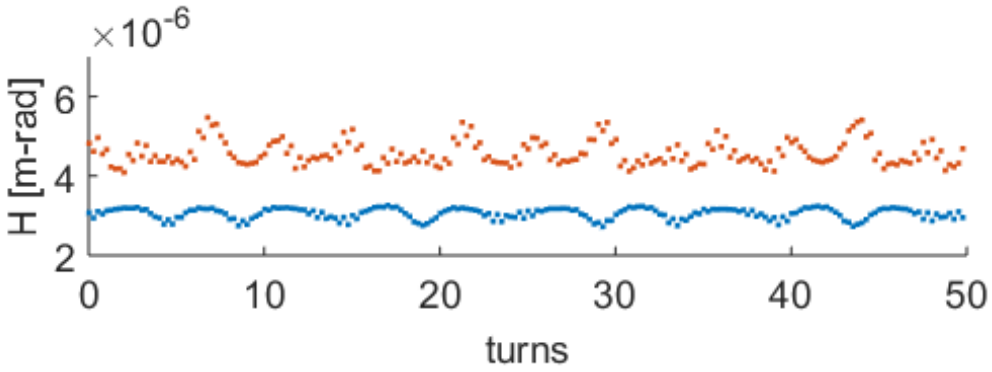

(b)

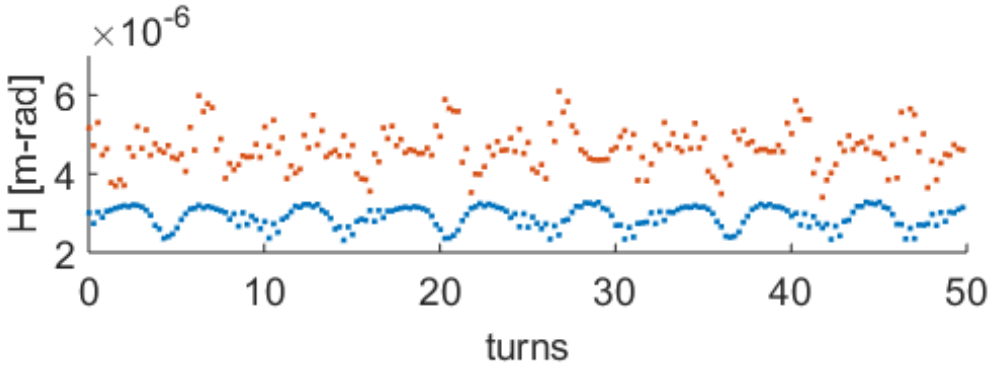

(c)

Fig. 6.5: Invariant H_N for N4 distributed lattice at $\nu_x = 4.13$, $\nu_y = 4.11$

Tab. 6.2: Results of invariant tracking in N4 octupole lattice.

$\nu_x = 4.13 \quad \nu_y = 4.11$			
I_{oct} [**A**]	$\langle H_N \rangle$	RMS variation	% variation peak-to-peak
0	3.22E-6	2.3E-8	2.4
0.5	3.17E-6	4.2E-8	6.2
2.0	3.05E-6	1.1E-7	17.6
4.0	2.91E-6	2.1E-7	33.5
$\nu_x = 3.88 \quad \nu_y = 3.83$			
I_{oct} [**A**]	$\langle H_N \rangle$	RMS variation	% variation peak to peak
0	2.92E-6	1.5E-8	2.3
0.5	2.90E-6	3.5E-8	6.8
2.0	2.82E-6	1.0E-7	20.8
4.0	2.93E-6	1.4E-7	59.9

tested 50 turns) may be possible. A natural extension of this work is to include predicted experimental errors into the invariant calculation, as well as extend consideration to a wider range of operating points.

6.2 Experimental Setup

The primary focus of this paper is the second consideration, an N4 distributed octupole lattice. The nonlinear inserts are comprised of 4 short octupoles distributed

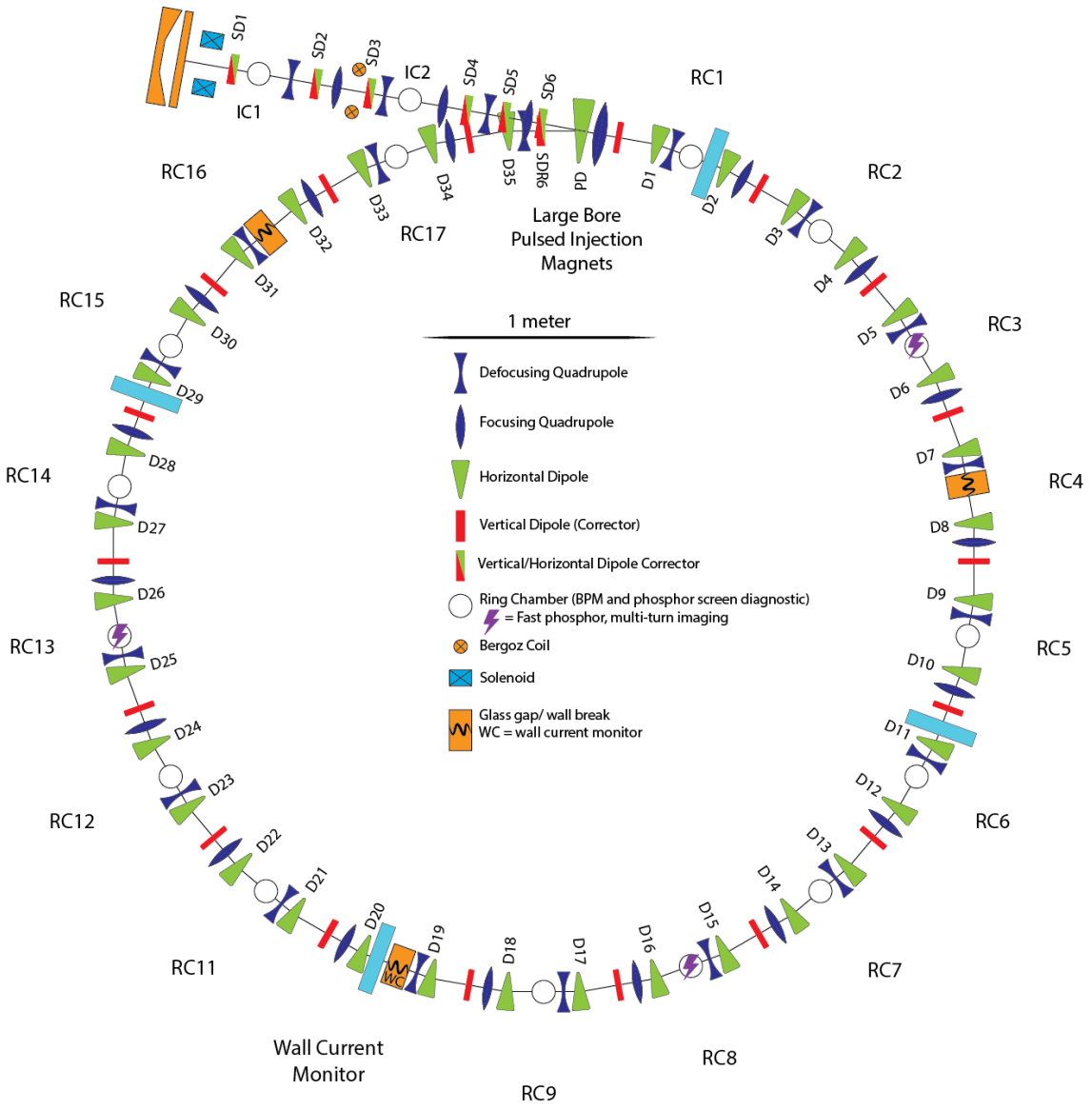

Fig. 6.6: N4 octupole lattice imposed on alternative lattice, large light-blue elements indicate octupole position.

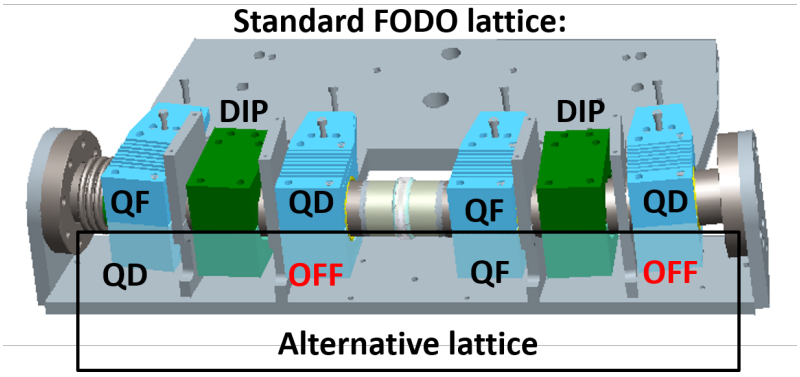

Fig. 6.7: Two standard UMER FODO cells (blue quadrupoles and green dipoles). In the Alternatice lattice, the crossed quadrupoles are unpowered, leaving a vacancy for octupole elements.

at even intervals about the ring (90^o points, see Fig. **??**). This configuration utilizes a mode of UMER operation known as the alternative lattice in which the total number of FODO cells in the ring is halved (by removing half of the quadrupoles). The two lattices are illustrated in Fig. 6.7. The nominal tune of the ring is also approximately halved, from $\nu \approx 6.7$ to ≈ 3.8. The alternative lattice uses printed circuit octupoles with the same aspect ratio as the standard UMER PC quad, which are seated in unused quadrupole mounts at the mid-point of the FODO cell.

The lattice can be tuned to have a tune of $4+\delta 2\pi$, where δ indicates the phase advance through the octupoles. For a turn length of 11.52 m, effective octupole length of 5.2 cm and tune near 4, the phase advance through the octupoles will be near $\psi = 0.07 * 2\pi$.

The N4 lattice is natively suited to the UMER structure, allowing the installation of octupoles with minimal disruptions to the ring (utilizing existing mounts

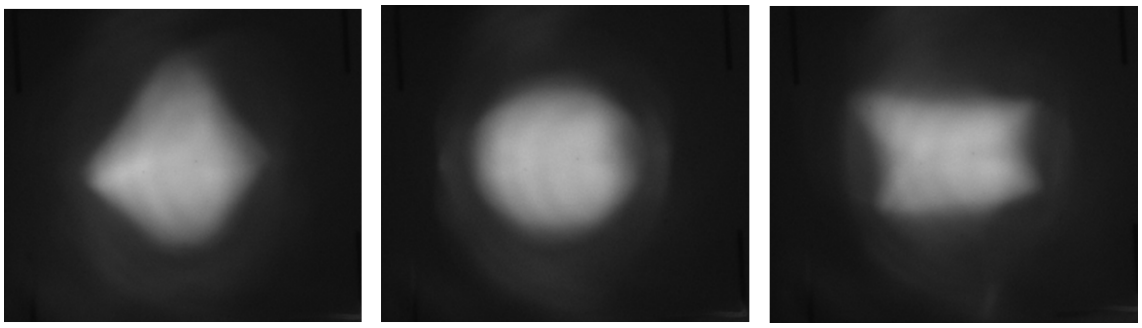

Fig. 6.8: Beam profile after 1 pass through octupole, imaged using phosphor screen. From left to right: $I_{oct} > 0$, $I_{oct} = 0$, $I_{oct} < 0$

and power supplies). However, it is a coarse approximation of the quasi-integrable octupole lattice and it is expected that these approximations will limit the extent to which the Hamiltonian H_N is conserved.

A key liberty taken with the quasi-integrable theory is the requirement that $\beta_x = \beta_y$ throughout the nonlinear element. In the N4 case, $\beta_x \approx \beta_y$, with differences on order 15%. The other approximation is that the PC octupole is fringe-dominated, meaning the longitudinal profile is not flat top and therefore the magnet cannot perfectly meet the requirement that $V_{oct} = 1/\beta^3 = \text{constant}$. Theoretical calculations of the UMER magnets predict that fringe fields cancel due to the relatively short magnet length. [**?**] It is yet to be seen if this cancellation will help preserve the nonlinear invariant. Octupole models used in simulations shown here utilize a hard-edged approximation.

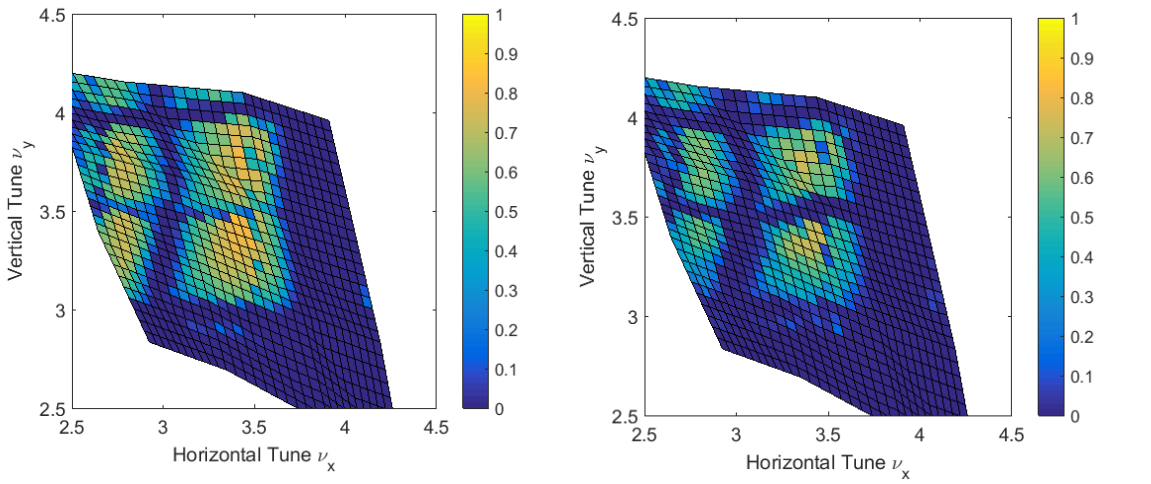

(a) Alternative lattice tune scan

(b) N4 lattice tune scan with octupoles powered at 0.5 A

Fig. 6.9: Tune scan data for 0.6 mA "pencil" beam, beam survival plot at 25 turns. Color axis is peak beam current normalized to 10th turn.

6.3 Preliminary Measurements

6.3.1 Tune Scan

In preparation for N4 lattice testing, measurements are taken on the alternative lattice to gauge beam losses over a variety of operating parameters. The tune scan technique, described in more detail in [**?**], measures variations in beam losses as a function of quadrupole strength in two families of quadrupoles (horizontally focusing and defocusing, notated as I_F and I_D). Fig. 6.9 shows beam survival measurements of the 0.6 mA beam for a range of quadrupole values. Transformation to tune-space was done using WARP simulations with hard-edged elements and a thin-lens model of dipole edge focusing. The obvious integer resonance bands are used to orient

the measurement in tune-space. An offset of $\nu_x = -0.45$ and $\nu_y = -0.35$ from the WARP prediction is necessary to line up integer bands.

The tunescan shows broad bands at the even integer tune resonances. As this N4 lattice is intended to be run at $\nu_x = \nu_y = 4 + \delta$, tuning the beam closer to this operating point will be necessary if any beneficial effect is to be observed over the integer band losses. With octupoles on (Figs. 6.9,6.8), no apparent increase in dynamic aperture is seen.

Errors: Beam Matching and Steering

The beam matching quadrupoles and steering correctors were optimized to a single operating point, at $I_F = I_D = 0.87$ A. It is expected that the accrued errors in the match and the steering grow with greater distance from the ideal operating point, although it is not clear that they accrue anisoptropically.

The steering solution for this operating point had first turn horizontal offsets in the quadrupoles of RMS 0.5 mm with a maximum of 1.3 mm. Vertically, RMS offsets are 3.2 mm with maximum value of approximately 8.5 +- 0.5 mm. The contribution of these steering errors can be seen in the width of the integer resonance bands in the tune scan data (Fig. **??**). More precise control of the steering will likely improve this characteristic by reducing the steering error for all operating points.

The beam match was not well-tuned, with percent RMS variations of 33% in the horizontal and 28% in the vertical. More accurate matching solutions have been demonstrated in UMER, up to standard deviations of 0.17 mm horizontally and 014 mm vertically for the 6 mA beam. [2]

6.4 Conclusion

In conclusion, UMER is equipped to test quasi-integrable octupole lattices. Insight has been built into the behavior of the N4 octupole lattice, which has potential to be a testbed for quasi-integrable dynamics. However, the proximity to an integer resonance band may ultimately limit its usefulness and implementation, at least with short octupole elements. On UMER, the large $\nu_x = 4$ band overshadows any resonant loss mitigation induced by the octupoles.

Bibliography

[1] V. Danilov and S. Nagaitsev. Nonlinear accelerator lattices with one and two analytic invariants. *Physical Review Special Topics - Accelerators and Beams*, 13(8):084002, aug 2010.

[2] Hao Zhang. *Experimental study of beam halo in intense charged particle beams*. PhD thesis, University of Maryland, College Park, 2014.